Int. J. Electrochem. Sci., 15 **(2020)** 5782 – 5792, doi: 10.20964/2020.06.26

International Journal of
ELECTROCHEMICAL
SCIENCE
www.electrochemsci.org

Synthesis of MnO_2/ZSM-5 Molecular Sieve Composites activated by CO_2 as Electrode Material for Supercapacitors

Xiaoling Lang[1,2,], Zhibiao Hu[1,2], Zhou Yunlong, Chenhao Zhao[1,2], TianFu Huang[1,2], Ningning Chen[3]*

[1] Fujian Provincial Key Laboratry of Clean Energy Materials, Longyan, Fujian, China 364000
[2] College of Chemistry & Materials Science, LongYan University, Longyan, Fujian, China 364012
3 Ecological Environment Monitoring Center, Binzhou, Shandong， China 256600
[*]E-mail: ahshio@163.com

Received: 9 January 2020 / *Accepted:* 9 March 2020 / *Published:* 10 May 2020

The high-performance electrode materials is a major issue in the development of large-scale supercapacitors. Here, we prepared a high capacity supercapacitor electrode material MnO_2/ZSM-5-CO_2 by CO_2 activated the support of molecular sieve (ZSM-5). The results show that the MnO_2/ZSM-5-CO_2 particles have obvious leafy structure, and uniform dispersed on the surface of the ZSM-5-CO_2. The specific capacitance of the MnO_2/ZSM-5-CO_2 materials is calculated to be 650.62 F g^{-1} higher than that of the ZSM-5-CO_2, MnO_2/ZSM-5-N_2. The MnO_2/ZSM-5-CO_2 electrode material, and also displayed great reversibility and stability long-term cycle life in repetitive charge-discharge cycling.

Keywords: MnO_2, molecular sieve, supercapacitor, CO_2 activation.

1. INTRODUCTION

Nowadays supercapacitors were attracted by more and more researchers' attention because of their stability cycle life and higher power density than batteries [1]. There are various application used supercapacitors owing to the great properties, such as burst power generation, public transportation and portable electronic devices. In supercapacitors, there are two kind of energy storage mechanism including the pseudo-capacitor and the electrical double-layer capacitor (EDLC) [2]. Regarding to the supercapacitors, the critical challenges mainly include low energy density that is determined by electrode materials and the high price. Currently most researchers mainly focused on the design of the electrode materials, like transition metal oxides, carbon and conducting polymers [3]. Manganese oxide (MnO_2) has been considered the most promising pseudo-capacitor electrode materials among various transition metal oxides owing to its high theoretical capacitance (1370 F g^{-1}), low price and good specific capacitance [4, 5]. However, the supercapacitors with MnO_2 electrode materials haven't presented the

excellent specific capacitance because of their poor electrical conductivity [6, 7]. In order to solve this problem, the mainly method is adding the other materials which have the good electrical conductivity, for example, CNTs, grapheme, carbon and ZnO to fabricate composite electrodes like CNTs-MnO_2 [8-10], MnO_2/carbon aerogel [11], Graphene oxide/MnO_2 [12, 13], ZnO/MnO_2 [14], MnO_2/Ni [15]. It is worthy to mention that regulating the morphology and structure of MnO_2 in favor of promoting the specific capacitance for supercapacitor [12]. Increasing the surface area, deducing the particle size and adjusting the porosity will benefit of improving the electrochemical performance of metal oxide as its active site increases [13].

ZSM-5 zeolite (Zeolite Socony Mobil-5) with Mobil Five structure have a highly regular 3 D structure, with high surface area， high porosity, and wide Si/Al ratios varying from 10 to several hundred [16,17]. ZSM-5 zeolites have been applied to the catalytic area many year such as gas sensor [18], Heterogeneous Fenton's oxidation [19], Photocatalytic degradation [20], electrocatalytic oxidation of methanol [21]. However, this has not report that ZSM-5 is applied on supercapacitors. In this study, a new compounds MnO_2/ZSM-5 have been synthesized and its application as a novel electrode materials for supercapacitors. In this work, CO_2 activation was applied for ZSM-5 (ZSM-5-CO_2) as the support of MnO_2 particles. CO_2 gas activation is a simple, safe and high efficient way to improve the microstructures of materials. CO_2 activation was usually applied for carbon materials, which impacts on their microstructures [22-24]. In this study, the surface morphologies of ZSM-5 support can be also considerably perfected by CO_2 activation. The microstructures and the electrochemical properties of the MnO_2/ZSM-5-CO_2 composites were characterized.

2. EXPERIMENTAL

2.1 Materials synthesis

The tube furnace should be followed nitrogen to remove air before the ZSM-5 material was activated under CO_2 at 950 ℃ for 1 h. When the tube furnace cooled down to room temperature, the obtained product was a gray powder denoted as ZSM-5-CO_2. A mixed solution was prepared by dissolving 0.30 g $MnCl.4H_2O$ and 0.16 g $KMnO_4$ in 40ml distilled water under vigorous stirring at room temperature. 0.6 g activated ZSM-5-CO_2 power was added into the above mixed solution, was then reflux heated 2 h, followed by filtration, and then dried at 80 ℃. The products were marked as MnO_2/ZSM-5-CO_2. For comparison, ZSM-5-N_2 was activated by the same method, but the gas was replaced with nitrogen. In this experiment all chemicals used were A. R. grade.

2.2 Materials characterization

The morphology and structure of catalysts were characterized by transmission electron microscopy (TEM) using a Tecnai G2 F30 S-Twin microscope (FEI, Netherlands) at a voltage of 200 kV and a current of 103 mA, coupled with energy dispersive X-Ray spectrometer (EDX, Thermo NORAN VANSTAGE ESI). The X-ray diffraction patterns (XRD, DX-2700, Dandong Fangyuan

Instrument Co., Ltd., China) were used to characterize the crystalline structure of the products with Cu K_α source operated at 45 kV. N_2 adsorption–desorption was examined by ASAP 2020 (Micromeritics, America) and the specific surface area of MnO_2/ZSM-5was measured by Brunauer–Emmett–Teller (BET) method.

2.3 Electrochemical measurements

The electrochemical performance of the MnO_2/ZSM-5 and the other materials were tested at a three electrode system at the 1 M Na_2SO_4 electrolyte, the working electrode was used the Ni foam coated with the prefabricated materials, the counter electrode was used the 1 cm^2 Pt foil, the reference electrode was used the saturated calomel electrode (SCE). The working electrode was prepared as following: 2.4 mg MnO_2/ZSM-5 or the other active materials, 0.3 mg polytetrafluoroethylene (PTFE) and 0.3 mg acetylene black were mixing in a mortar, and then added 0.5 ml ethanol. After mixing several times, the above slurries were coated on Ni foam. Finally the mixture was dried at 60 ℃ for 12h. The cyclic voltammograms (CV) and Charge-discharge curves were tested on a CHI 660C electrochemistry workstation at room temperature in 1 M Na_2SO_4 electrolyte. The long-term cycling performances were recorded on BTS battery test system (Shenzhen, China).

3. RESULTS AND DISCUSSION

The XRD patterns of ZSM-5, ZSM-5-N_2 and ZSM-5-CO_2 samples are shown in Fig. 1. It can be found that the three samples are all demonstrated the main diffraction peaks of ZSM-5 zeolite at 14.1°, 14.9°, 16.0°, 23.4°, 24.2°, 30.5°, 45.5°. This result is consisted with the reference samples [20, 21]. The XRD diffraction result shows that the ZSM-5 materials treated by different methods have the similar crystal frames of ZSM-5, and illustrated that active treated haven't change the crystal structure of ZSM-5. Fig. 2 displays the XRD patterns of the ZSM-5-CO_2 and MnO_2/ZSM-5-CO_2 samples. It is obvious that both the two samples have the typical diffraction peak of ZSM-5. The peak at the 36.7°, 42.2°, 54.9° and 66.3° are corresponding to the (100), (101), (102) and (110) planes of MnO_2 confirming that MnO_2 crystallines were loaded on ZSM-5 successfully. In addition the diffraction peaks of MnO_2 is not very obvious in Fig.2. May be the reason for this is that the size of MnO_2 particles are smaller.

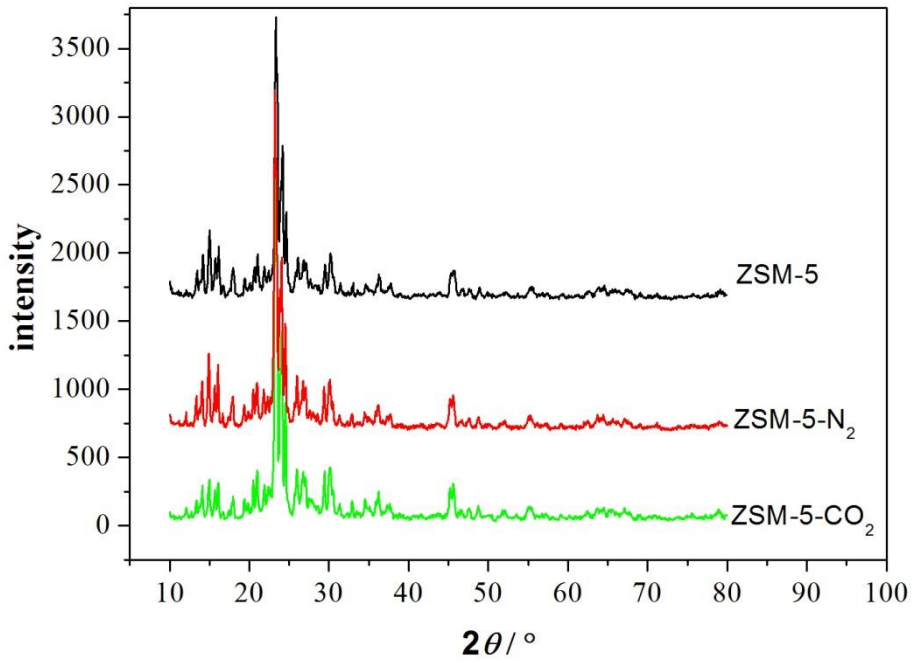

Figure 1. XRD patterns of the ZSM-5, ZSM-5-N_2 and ZSM-5-CO_2 particles.

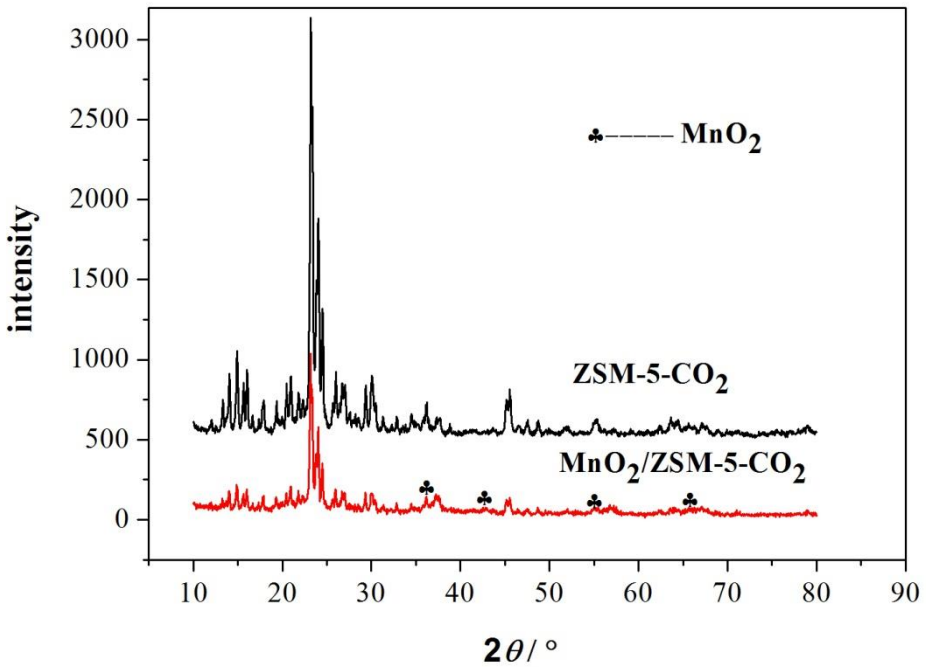

Figure 2. XRD patterns of the ZSM-5-CO_2 and MnO_2/ZSM-5-CO_2 particles.

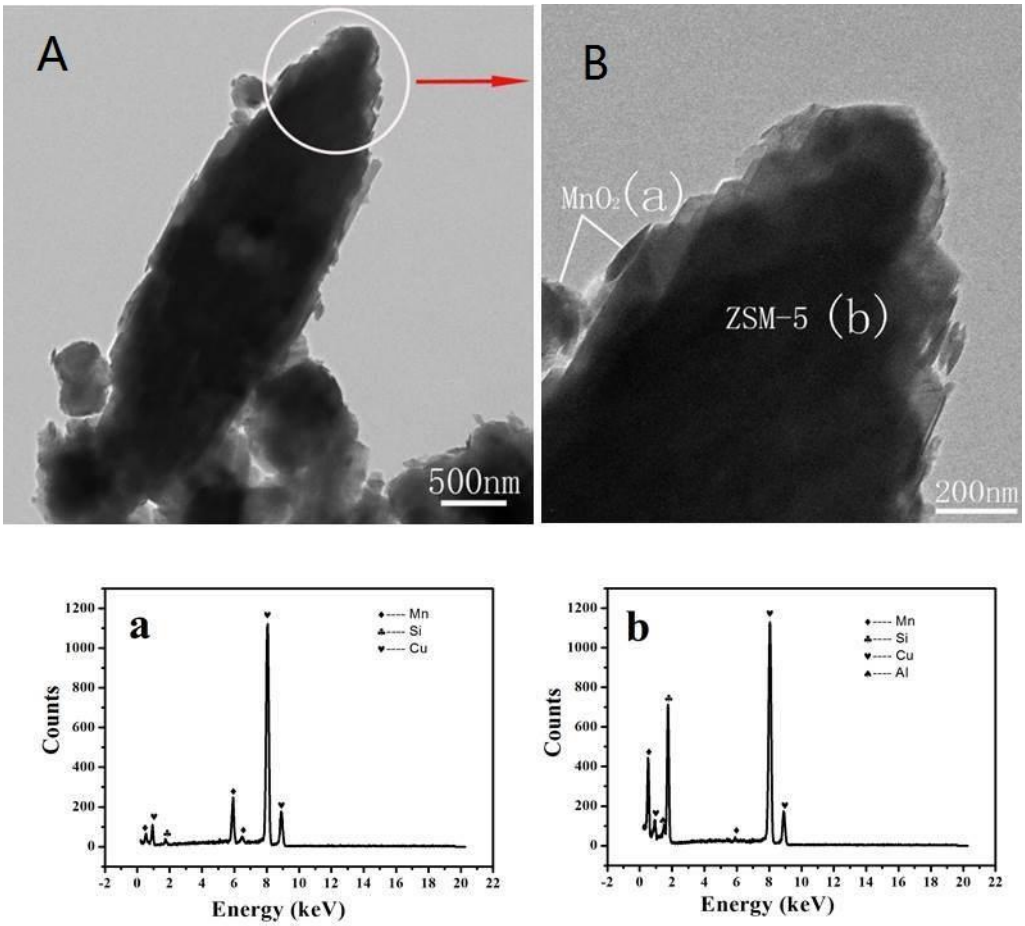

Figure 3. TEM image of MnO_2/ZSM-5-CO_2 particle (A, B) and EDS patterns of (a) Part a and (b) Part b in the TEM image B

The structural and morphological characteristics of MnO_2/ZSM-5-CO_2 materials are observed by TEM, as shown in Fig. 3. The results show that the MnO_2/ZSM-5-CO_2 particles have obvious leafy structure, and the MnO_2 are dispersed on the surface of the ZSM-5-CO_2 (Fig. 3A and B). The EDS analysis (Fig. 3a, b) for the edge of the MnO_2/ZSM-5-CO_2 (a) indicates the most element of Mn while the minor Si elements, and the surface consist of Mn, Si and Al elements. The result shows that MnO_2 can finely dispersed on the surface of the ZSM-5 by a simple treatment with CO_2 activation.

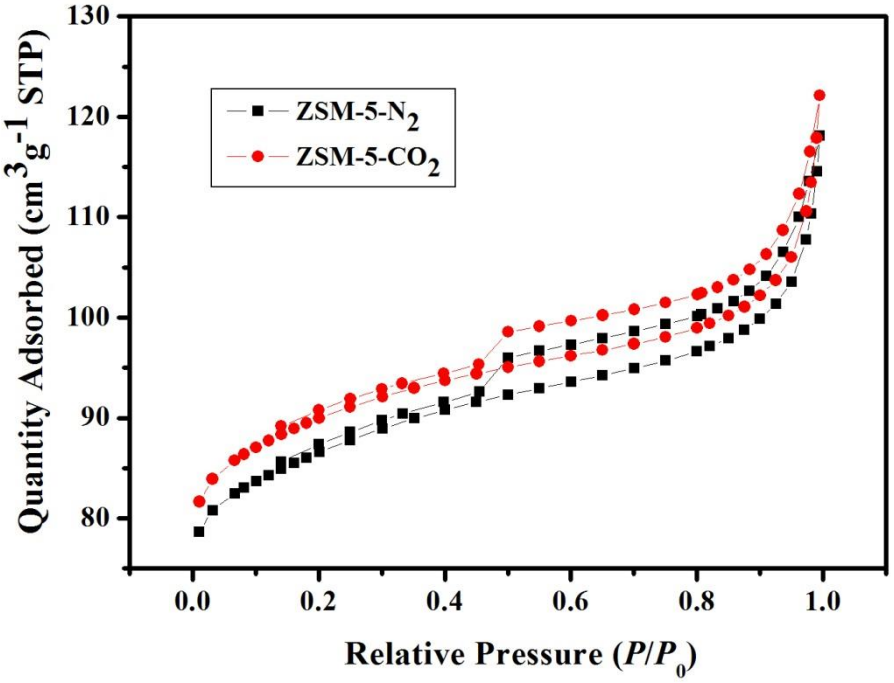

Figure 4. The nitrogen adsorption/desorption isotherm of ZSM-5-N_2 and ZSM-5-CO_2 particles.

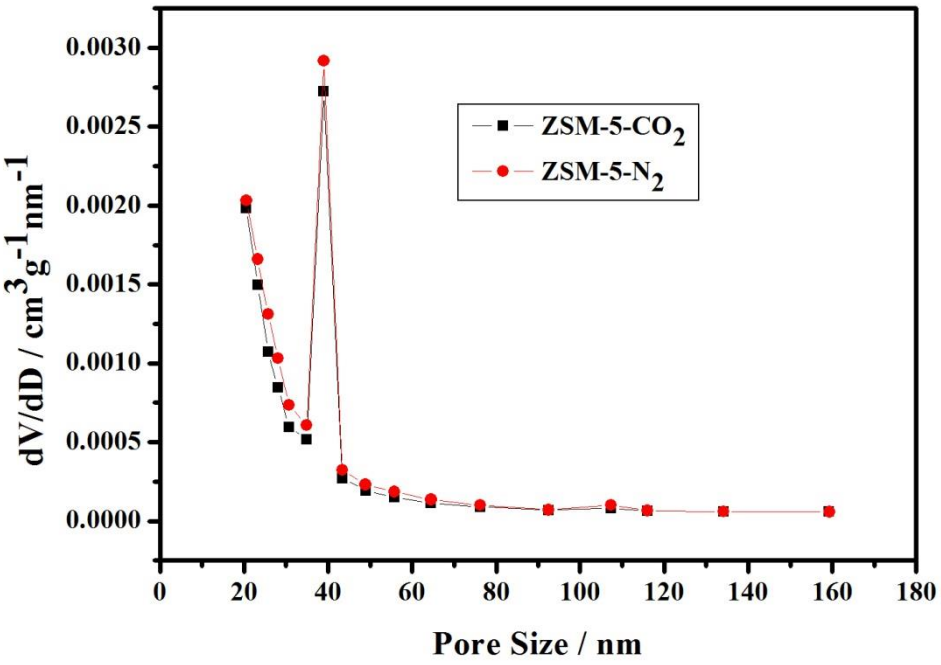

Figure 5. Pore size distribution curves of ZSM-5-N_2 and ZSM-5-CO_2 particles.

As shown in Fig. 4, the ZSM-5-N_2 and ZSM-5-CO_2 materials both exhibit typical type IV curves with pressure increasing, and the isotherm shows a sharp increase in the amount of adsorption followed by saturation, so there is a hysteresis between adsorption and desorption branches. Therefore, this typical

type IV curves illustrate that the ZSM-5-N_2 and ZSM-5-CO_2 materials both have the characteristics of mesoporous structure [13]. Fig. 5 gives the results of pore size distribution of the ZSM-5-N_2 and ZSM-5-CO_2 samples. It is indicates that pore size distribution of two materials almost concentrated in the 40 nm. And the narrow pore size distribution curve shows that the ZSM-5-N_2 and ZSM-5-CO_2 materials have a mesostructure with uniform mesopores. The BET surface area of ZSM-5-CO_2 calculated from data at the lower N_2 pressures is about 313.09 m^2/g higher than the BET surface area of 190.93 m^2/g for ZSM-5-N_2. It is worth to notice that the CO_2 activation processes may play an important role in controlling the structure of ZSM-5 zeolite.

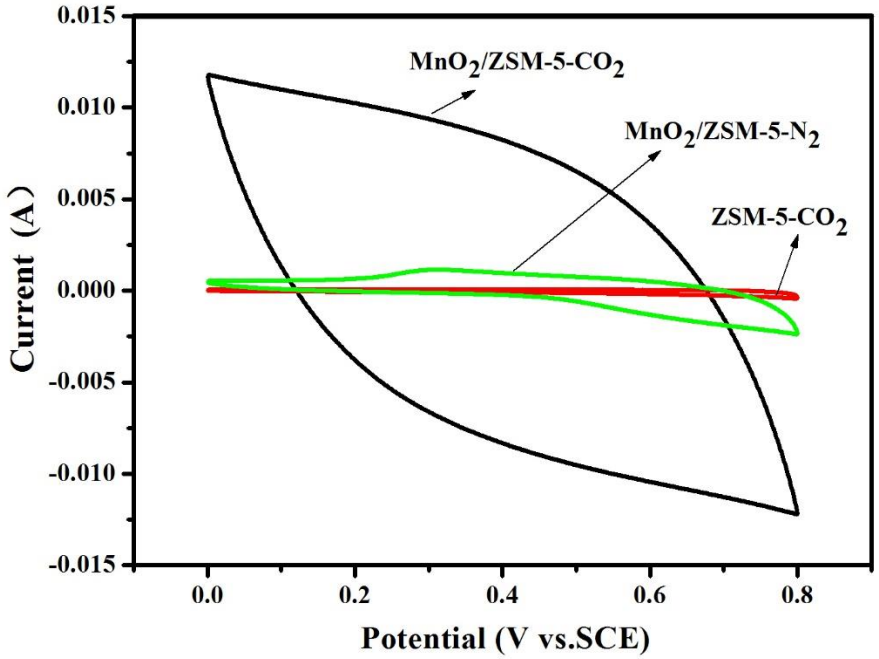

Figure 6. Cyclic voltammograms of ZSM-5-CO_2, MnO_2/ZSM-5-N_2 and MnO_2/ZSM-5-CO_2 materials in 1 M Na_2SO_4 electrolyte.

The electrochemical behaviors of the ZSM-5-CO_2, MnO_2/ZSM-5-N_2 and MnO_2/ZSM-5-CO_2 materials were performed by cyclic voltammetry (CV) at the scan rate of 50 mV s^{-1} in 1M Na_2SO_4 aqueous electrolyte. As show in Fig.6, the MnO_2/ZSM-5-CO_2 composite has a larger integral area of the CV cure compare to ZSM-5-CO_2 and MnO_2/ZSM-5-N_2. This result demonstrates that the MnO_2/ZSM-5-CO_2 material shows a higher specific capacitance, the reason may be attributed to the increased specific surface area by the CO_2 activation of the ZSM-5. The ion can easy to transport from the active materials to electrolyte, and the great electrical conductivity can improve the electron transfer in the faradic capacitance behavior owing to the large surface area of the active materials [25].

To further investigate the electrochemical performance of ZSM-5-CO_2, MnO_2/ZSM-5-N_2 and MnO_2/ZSM-5-CO_2 materials, galvanostatic charge/discharge curves were tested in 1 M Na_2SO_4

electrolyte in a voltage range of 0 - 0.8 V at 1 A g^{-1} current density. Fig. 7 shows the charge/discharge curves of ZSM-5-CO_2, MnO_2/ZSM-5-N_2 and MnO_2/ZSM-5-CO_2 all are closely linear and illustrate an obvious triangle distribution indication a great capacitive performance [26]. In addition, all the charge/discharge curves haven't the obvious voltage drop at the galvanostatic charge/discharge current switches. It is illustrate that a quite low resistance of the ZSM-5-CO_2, MnO_2/ZSM-5-N_2 and MnO_2/ZSM-5-CO_2 electrode. The specific capacitance of the electrode materials can be calculated according to Equation [27] (1):

$$C = \frac{I\Delta t}{m\Delta V} \qquad (1)$$

C: the specific capacitance (F g^{-1});
I: the charge-discharge current (A);
Δt: the discharge time (s);
ΔV: the voltage (V);
m: the mass of the active materials (g);

The specific capacitance of the ZSM-5-CO_2, MnO_2/ZSM-5-N_2 and MnO_2/ZSM-5-CO_2 materials is calculated to be 6.25, 72.27, 650.62 F g^{-1} respectively. It is suggest that the MnO_2/ZSM-5-CO_2 composite has the highest specific capacitances. The result is agreed with the CV result. It can be explained that MnO_2/ZSM-5-CO_2 composite had the larger specific surface areas and increased active sites because the ZSM-5 was treatment with CO_2 activation.

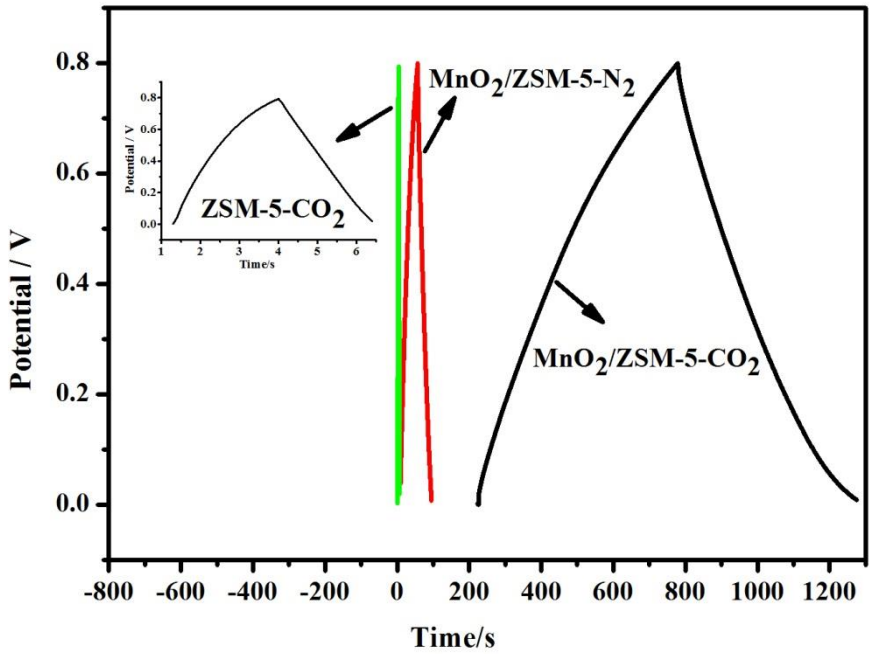

Figure 7. Charge-discharge curves of ZSM-5-CO_2, MnO_2/ZSM-5-N_2 and MnO_2/ZSM-5-CO_2 materials in 1 M Na_2SO_4 electrolyte.

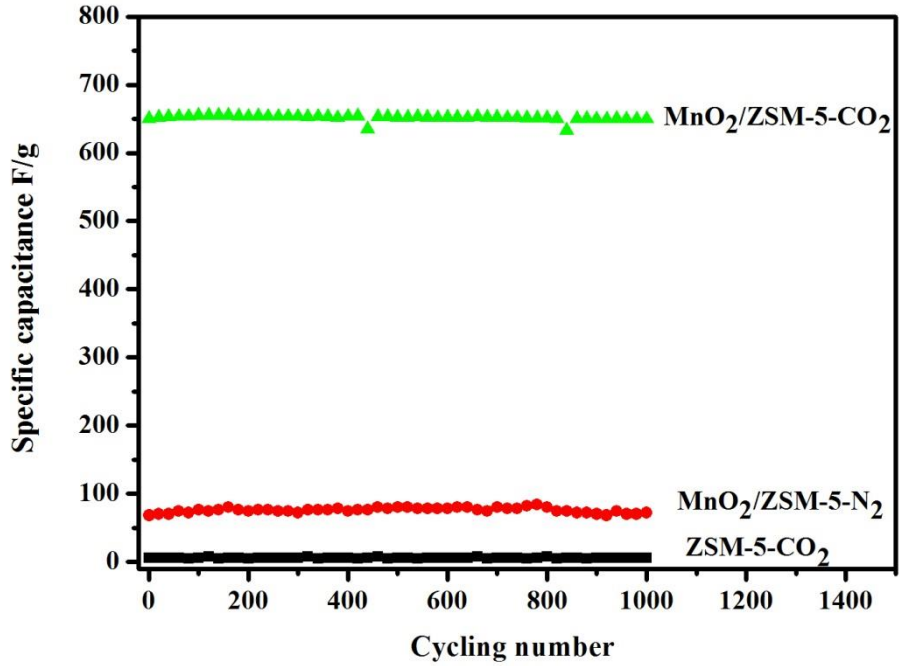

Figure 8. Cycling performances of ZSM-5-CO_2, MnO_2/ZSM-5-N_2 and MnO_2/ZSM-5-CO_2 materials in 1 M Na_2SO_4 electrolyte.

Long-term cycling performance of active materials is an important parameter for the supercapacitors [28]. In order to evaluate the stability of ZSM-5-CO_2, MnO_2/ZSM-5-N_2 and MnO_2/ZSM-5-CO_2 materials, the cycling performances were recorded and the results are shown in Fig.8. The MnO_2/ZSM-5-CO_2 composite has the highest specific capacitance after 1000 cycles. In addition, the specific capacitance of the MnO_2/ZSM-5-CO_2 composite also show the good retention of about 100% after 1000 cycles, demonstrating that the MnO_2/ZSM-5-CO_2 electrode shows a good long-term cycle stability and a great reversibility during the repetitive charge-discharge cycling test.

In order to prove the electrochemical activity of MnO_2/ZSM-5-CO_2, we compared the specific capacitance of several MnO_2 from different reference. The results are listed in Table 1, which show that the specific capacitance of MnO_2/ZSM-5-CO_2 has the highest value than the other MnO_2/ electrode materials. It can be explained that MnO_2/ZSM-5-CO_2 composite has more active sites owing to the ZSM-5 is treated with CO_2 activation.

Table 1. Comparison the MnO_2 electrode materials of specific capacitance between different references

Electrode Material	Specific Capacitance	Electrolyte	Ref
MnO_2/ZSM-5-CO_2	650.62 F g^{-1}	Na_2SO_4	This work
MnO_2-NF	194.6 F g^{-1}	Na_2SO_4	[29]
graphene/MnO_2	380 F g^{-1}	Na_2SO_4	[30]
MnO_2/CNT	179 F g^{-1}	Na_2SO_4	[31]
graphene/MnO_2	465 F g^{-1}	Na_2SO_4	[32]
Graphene-MnO_2	310 F g^{-1}	Na_2SO_4	[33]

4. CONCLUSION

Herein, we develop a high capacity supercapacitor electrode material MnO_2/ZSM-5-CO_2 by CO_2 activated the support of ZSM-5. The influences of CO_2 activation on the structure and electrochemical performances of MnO_2/ZSM-5 are researched. The MnO_2/ZSM-5-CO_2 particles have obvious leafy structure, and the MnO_2 particles are dispersed on the surface of the ZSM-5-CO_2. The specific capacitance of the MnO_2/ZSM-5-CO_2 materials is calculated to be 650.62 F g^{-1} higher than that of the ZSM-5-CO_2, MnO_2/ZSM-5-N_2. The MnO_2/ZSM-5-CO_2 electrode also exhibited a good long-term cycle stability and a great reversibility during the repetitive charge-discharge cycling test. It can be explained that MnO_2/ZSM-5-CO_2 composite has the larger specific surface areas and more active sites because the ZSM-5 is treated with CO_2 activation.

ACKNOWLEDGEMENT
The authors thank the financial supports from the Science and Technology Program of Longyan (2018LYF8010), the Natural Science Foundation of Fujian Province (2019J01800), and the Qimai Natural Science Foundation of Shanghang County (2018SHQM01).

References

1. D. Guo, Y. Luo, X. Yu, *Nano Energy*, 8 (2014) 174.
2. T. Nguyen, M. Boudard, M.J. Carmezim, *Energy*, 126 (2017) 208.
3. D. Xiang, L. Yin, C. Wang, *Energy*, 106 (2016) 103.
4. Y.L. Zhou, Y.S. Jiang, Z.B. Hu, *Int. J. Electrochem. Sci.*, 14 (2019) 5396.
5. H.L. Xu, Q. Cao, X.Y. Wang, *Materials Science and Engineering: B*, 171 (2010) 104.
6. J.K. Chang, M.T. Lee, W.T. Tsai, *J. Power Sources*, 166 (2007) 590.
7. S. Devaraj, N. Munichandraiah, *J. Phys. Chem. C*, 112 (2008) 4406.
8. A.L.M. Reddy, M.M. Shaijumon, S.R. Gowda, P.M. Ajayan, *J. Phys. Chem. C*, 114 (2010) 658.
9. M. Toupin, T. Brousse, D. Belanger, *Chem. Mat.*, 16 (2004) 3184.
10. V. Subramanian, H.W. Zhu, B.Q. Wei, *Electrochem. Commun.*, 8 (2006) 827.
11. Q. Li, J.M. Andersonc, Y. Chen, *Electrochim. Acta*, 59 (2012) 548.
12. S.W. Lee, J. Kim, S. Chen, *ACS Nano*, 4 (2010) 3889.
13. J. Li, X.Y. Wang, Q.H. Huang, *J. Power Sources*, 160 (2006) 1501.
14. S. Chen, J.W. Zhu, X.D. Wu, *ACS Nano*, 4 (2010) 2822.
15. K. Dai, L. Lu, C. Liang, *Electrochim. Acta*, 116 (2014) 111.
16. Y.B. He, G.R. Li, Z.L. Wang, *Energy Environ. Sci.*, 4 (2011) 1288.
17. K. Xiao, J.W. Li, G.F. Chen, *Electrochim. Acta*, 149 (2014) 341.
18. M. Hartmann, S. Kullmanna, H. Keller, *J. Mater. Chem.*, 20 (2010) 9002.
19. F. Duarte, L.M. Madeira, *Sep. Sci. Technol.*, 45 (2010) 1512.
20. A. Dubbe, *Sensors Actuat. B*, 137 (2009) 205.
21. S. Queiros, V. Morais, S.D. Carmen, *Sep. Purif. Technol.*, 141 (2015) 235.
22. C.T. Chang, J.J. Wang, T. Ouyang, *Materials Science and Engineering B*, 196 (2015) 53.
23. J.B. Raoof, N. Azizi, R. Ojani, *Int. J. Hydrogen Energ.*, 36 (2011) 13295.
24. N. Liu, J. Shen, D. Liu, *Micropor. Mesopor. Mat.*, 167 (2013) 176.
25. D. Liu, J. Shen, N.P. Liu, *Electrochim. Acta*, 89 (2013) 571.
26. E.J. Lee, Y.J. Lee, J.K. Kim, *Mater. Res. Bull.*, 70 (2015) 209.
27. F.Y. Cheng, J. Liang, Z.L. Tao, *Adv. Mater.*, 23 (2011) 1695.

28. B. Zhao, P. Liu, Y. Jiang, *J. Power Sources*, 198 (2012) 423.
29. H.G. Gao, F. Xiao, C.B. Ching, H.W. Duan, *ACS Appl. Mater. Interfaces*, 4 (2012) 2801.
30. G.H Yu, L.B Hu, N. Liu, H.L. Wang, M. Vosgueritchian, Y. Yang, Y. Cui, Z.N. Bao, *Nano Lett.*, 11 (2011) 4438.
31. L. Demarconnay, E. Raymundo-Pinero, F. Béguin, *J. Power Sources*, 196 (2011) 580.
32. Y.M. He, W.J. Chen, X.D. Li, Z.X. Zhang, J.C. Fu, C.H. Zhao, E.Q. Xie, *ACS. Nano*, 7 (2013) 174.
33. J. Yan, Z.J. Fan, T. Wei, W.Z. Qian, M.L. Zhang, F. Wei, *Carbon*, 48 (2010) 3825.